

Water-Soluble, Isolable Gold Clusters Protected by Tiopronin and Coenzyme A Monolayers

Allen C. Templeton, Shaowei Chen, Stephen M. Gross, and Royce W. Murray*

Venable and Kenan Laboratories of Chemistry, University of North Carolina,
Chapel Hill, North Carolina 27599-3290

Received July 8, 1998. In Final Form: November 2, 1998

Isolable, water-soluble gold clusters protected by monolayers of tiopronin (tiopronin-MPCs) or coenzyme A (CoA-MPCs) were synthesized by a procedure of comparable simplicity to the Brust synthesis for alkanethiolate monolayer-protected gold clusters. High-resolution transmission electron microscopy shows that, like their alkanethiolate-MPC counterparts, the average core diameters of tiopronin-MPCs can be systematically controlled by varying the tiopronin: Au mole ratio employed in the reaction. The UV-vis spectra of tiopronin-MPCs exhibit pH and core size dependency of the surface plasmon band position and intensity, respectively. Thermogravimetric analysis of the tiopronin-MPCs gave average numbers of tiopronin ligands per cluster; for example, tiopronin-MPCs with an average core size of 1.8 nm ($\sim\text{Au}_{201}$) are protected with an average of 85 tiopronin ligands. ^1H NMR reveals a size-dependent evolution of spectral features interpreted as reflecting differences in attachment sites (terrace, defects) and/or restriction in ligand mobility. Infrared spectroscopy reveals strong hydrogen bonding in the monolayer and provides evidence for intercluster association, and acid/base titrations produce $\text{p}K_{\text{A}}$ values similar to the free ligand in the presence of a charge-screening supporting electrolyte, but higher in its absence. The same analytical methods were also applied to CoA-MPCs.

Nanometer-sized metallic and semiconducting particles have been the subject of substantial research attention over the last two decades.¹ Because such materials represent an "intermediate" dimension between bulk materials and small molecules, they offer potential for generating unusual chemical, electronic, and physical properties.² While numerous routes exist for the production of colloidal gold particles,³ the description by Brust et al.⁴ of nanometer-sized alkanethiolate monolayer-protected gold clusters (alkanethiolate-MPCs) paved the way to materials with properties akin to those of large, robust molecules, namely, stability in air and in solvent-free forms and ease of characterization by standard analytical techniques.⁵ Most importantly from the chemist's viewpoint, it has been demonstrated that these nanoparticles can be functionalized with a wide variety of structural units using simple chemical transformations.^{6–10}

Following the initial⁴ synthetic report and subsequent characterizations, we and others have elucidated a number of additional important features of alkanethiolate-MPCs: (a) The $\text{RSH}:\text{AuCl}_4^-$ mole ratio governs the average core size produced in the synthesis, which is appealing for examining the size dependence of important physical and chemical properties.^{5b,11} (b) The crude synthetic MPC product is modestly polydisperse (in core size) but can be separated into rather monodisperse samples by fractional precipitation.¹² Electrochemistry of room-temperature solutions of monodisperse clusters exhibits quantized capacitive (Coulomb staircase) charging steps and further displays a transition from metal-like to molecule-like core charging characteristics with decreasing MPC core size.¹³ (c) Cluster functionalization can be achieved by simple place-exchange reactions with ω -functionalized alkanethiolates, providing a path to explore clusters functionalized with multiple electroactive moieties.^{6–8} (d) The coupling reactivity of ω -functionalized alkanethiolate/Au MPCs has been demonstrated,^{9,10} expanding the scope of MPCs available as large, polyfunctional chemical reagents that are in many ways analogous to dendrimers and hyperbranched polymers.¹⁴

* Corresponding author's e-mail address: rwm@email.unc.edu.

(1) Schmid, G. *Clusters and Colloids. From Theory to Applications*; VCH: New York, 1994. (b) Haberland, H., Ed. *Clusters of Atoms and Molecules*; Springer-Verlag: New York, 1994.

(2) Schon, G.; Simon, U. *Colloid Polym. Sci.* **1995**, *273*, 101–117, 202–218. (b) Mayya, K. S.; Sastry, M. *Langmuir* **1998**, *14*, 74–78. (c) Vossmeier, T.; Katsikas, L.; Giersig, M.; Popovic, I. G.; Diesner, K.; Chemseddine, A.; Eychmuller, A.; Weller, A. *J. Phys. Chem.* **1994**, *98*, 7665–7673. (d) Nosaka, Y.; Ohta, N.; Fukuyama, T.; Fuhii, N. *J. Colloid Interface Sci.* **1993**, *155*, 23–29. (e) Hayes, D.; Meisel, D.; Micic, O. I. *Colloids Surf.* **1991**, *55*, 121–126.

(3) Hayat, M. A., Ed. *Colloidal Gold: Principles, Methods, and Applications*; AP: New York, 1989; Vol. 1.

(4) Brust, M.; Walker, M.; Bethell, D.; Schiffrin, D. J.; Whyman, R. *J. Chem. Soc., Chem. Commun.* **1994**, 801–802. (b) Brust, M.; Fink, J.; Bethell, D.; Schiffrin, D. J.; Kiely, C. *J. Chem. Soc., Chem. Commun.* **1995**, 1655–1656.

(5) For a recent review, refer to: Hostetler, M. J.; Murray, R. W. *Curr. Opin. Colloid Interface Sci.* **1997**, *2*, 42–50. (b) Hostetler, M. J.; Wingate, J. E.; Zhong, C.-J.; Harris, J. E.; Vachet, R. W.; Clark, M. R.; Londono, J. D.; Green, S. J.; Stokes, J. J.; Wignall, G. D.; Glish, G. L.; Porter, M. D.; Evans, N. D.; Murray, R. W. *Langmuir* **1998**, *14*, 17–30.

(6) Hostetler, M. J.; Green, S. J.; Stokes, M. J.; Murray, R. W. *J. Am. Chem. Soc.* **1996**, *118*, 4212–4213.

(7) Ingram, R. S.; Hostetler, M. J.; Murray, R. W. *J. Am. Chem. Soc.* **1997**, *119*, 9175–9178. (b) Ingram, R. S.; Murray, R. W. *Langmuir* **1998**, *14*, 4115–4121.

(8) Green, S. J.; Stokes, J. J.; Hostetler, M. J.; Pietron, J. J.; Murray, R. W. *J. Phys. Chem. B* **1997**, *101*, 2663–2668. (b) Green, S. J.; Pietron, J. J.; Stokes, J. J.; Hostetler, M. J.; Vu, H.; Wuelfing, W. P.; Murray, R. W. *Langmuir* **1998**, *14*, 5612–5619.

(9) Templeton, A. C.; Hostetler, M. J.; Kraft, C. T.; Murray, R. W. *J. Am. Chem. Soc.* **1998**, *120*, 1906–1911.

(10) Templeton, A. C.; Hostetler, M. J.; Warmoth, E. K.; Chen, S.; Hartshorn, C. M.; Krishnamurthy, V. M.; Forbes, M. D. E.; Murray, R. W. *J. Am. Chem. Soc.* **1998**, *120*, 4845–4849.

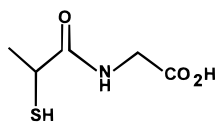
(11) Leff, D. V.; Ohara, P. C.; Heath, J. R.; Gelbart, W. M. *J. Phys. Chem.* **1995**, *99*, 7036–7041.

(12) Whetten, R. L.; Khoury, J. T.; Alvarez, M. M.; Murthy, S.; Vezmar, I.; Wang, Z. L.; Stephens, P. W.; Cleveland, C. L.; Luedtke, W. D.; Landman, U. *Adv. Mater.* **1996**, *8*, 428–433.

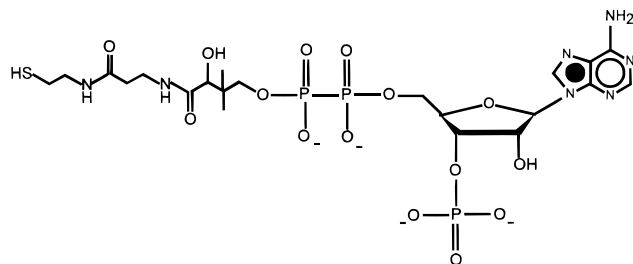
(13) Ingram, R. S.; Hostetler, M. J.; Murray, R. W.; Schaaff, T. G.; Khoury, J. T.; Whetten, R. L.; Bigioni, T. P.; Guthrie, D. K.; First, P. N. *J. Am. Chem. Soc.* **1997**, *119*, 9279–9280. (b) Chen, S.; Ingram, R. S.; Hostetler, M. J.; Pietron, J. J.; Murray, R. W.; Schaaff, T. G.; Khoury, J. T.; Alvarez, M. M.; Whetten, R. L. *Science* **1998**, *280*, 2098–2101.

The present research was inspired by the fact that alkanethiolate-MPCs are insoluble in water, and while place-exchanged MPCs bearing polar ω -functionalities dissolve in several polar solvents, none has proven to be water soluble. Monolayer-protected gold clusters have been discussed^{4,5a} in the context of nanoscale electronic devices, multifunctional catalysts, and chemical sensors. Potential applications also exist in biological chemistry, including biosensors based, for example, on binding reactions with clusters functionalized with receptor and/or reporter sites,³ and as materials useful in the emerging field of biolistics.¹⁵ Access to these and other applications would be facilitated by a wide range of MPC solubility properties, including water solubility. The important questions that begin to be addressed in this study are: Can water-soluble MPCs containing nanometer-sized metal cores be prepared by routes as facile as the Brust method?⁴ Can the monolayer functionality of such water-soluble MPCs be manipulated by place-exchange and coupling chemistry like those of their alkanethiolate-MPC relatives? Can polydispersities in core size and place-exchanged ligands be resolved as a function of core size and ligand identity?

MPCs having partially or fully ω -carboxylic acid functionalized alkanethiolate ligand shells (and related examples) are^{9,16} soluble in polar solvents such as ethanol and acetone but exhibit sparing to negligible solubility in water. This behavior suggests that water solubility must be sought by minimizing (or eliminating) the methylene spacer content and by including polar elements between the thiol group and ω -terminal sites. Examples that meet these requirements are thiol-containing biomolecules such as tiopronin and coenzyme A.



TIOPRONIN



COENZYME A

Tiopronin (*N*-2-mercaptopropionylglycine) is a pharmaceutically important drug used for the treatment of cystinuria and rheumatoid arthritis.¹⁷ Importantly, tiopronin has a free terminal $-\text{CO}_2\text{H}$ group which provides a handle for further reactivity, acidity, and ion-exchange separation studies with tiopronin monolayer-protected Au clusters. Coenzyme A, a naturally occurring enzyme cofactor important in the mediation of acyl transfer in biological organisms,¹⁸ yields a monolayer substantially

more complex than that of tiopronin. This material is attractive because enzymatic pathways in which the monomer is known to participate have the potential to be harnessed for using CoA-MPCs in the construction of biomaterial interfaces.

This paper describes the synthesis and characterization of MPCs based on protecting monolayers composed solely of tiopronin (tiopronin-MPCs) and coenzyme A (CoA-MPCs). MPC core sizes comparable to those of the Brust method⁴ (e.g., alkanethiolate-MPCs) are obtained by two slightly different routes: for CoA-MPC synthesis, a CoASH/AuCl₄⁻ mixture was reduced in H₂O, and for tiopronin-MPC synthesis, a tiopronin/AuCl₄⁻ mixture was reduced in a 6:1 methanol/acetic acid solution. As in the Brust reaction,⁴ core size varies systematically with the ligand:AuCl₄⁻ mole ratio employed in the reaction.^{5b,11} The tiopronin- and CoA-MPCs are characterized with high-resolution transmission electron microscopy (HRTEM), thermogravimetric analysis (TGA), NMR, UV-vis, FTIR, and acid/base titrations.

Experimental Section

Chemicals. HAuCl₄·xH₂O was either purchased (Aldrich, 99.99%) or synthesized according to the literature.¹⁹ *N*-(2-Mercaptopropionyl)glycine (tiopronin, 99%) and sodium borohydride (99%) were purchased from Aldrich, and coenzyme A (extracted from yeast) was purchased from Sigma (92%). Water was purified by passing house-distilled water through a Barnstead NANOpure system (≥ 18 M Ω). All other chemicals were reagent grade and used as received.

Synthesis of Tiopronin Monolayer-Protected Clusters.

In a typical reaction, 0.31 g of tetrachloroauric acid (0.80 mmol) and 0.38 g of *N*-(2-mercaptopropionyl)glycine (2.4 mmol) were codissolved in 35 mL of 6:1 methanol/acetic acid, giving a ruby red solution. NaBH₄ (0.6 g, 16 mmol) in 15 mL of H₂O was added with rapid stirring, whereupon the solution temperature immediately rose from 24 °C (room temperature) to 44 °C (returning to room temperature in ca. 15 min). Meanwhile, the solution pH increased from its initial 1.2 value to 5.1. The black suspension that was formed was stirred for an additional 30 min after cooling, and the solvent was then removed under vacuum at ≤ 40 °C.

Two aspects of the reaction conditions were varied as part of this study (Table 1): (a) the initial solution temperature, before addition of NaBH₄ reductant, and (b) the mole ratio of tiopronin to HAuCl₄·xH₂O employed.

The crude tiopronin-MPC is completely insoluble in methanol but quite soluble in water. It was purified by dialysis, in which the pH of 150 mg of crude product dissolved in 75 mL of water (NANOpure) was adjusted to 1 by dropwise addition of concentrated HCl. This solution was loaded into 8 in. segments of cellulose ester dialysis membrane (Spectra/Por CE, MWCO = 10 000), placed in 4 L beakers of water (NANOpure), and stirred slowly, recharging with fresh water ca. every 10 h over the course of 72 h. The dark blue tiopronin-MPC solutions were collected from the dialysis tubes, and the solvent was removed under vacuum at ≤ 40 °C. The product materials were found to be spectroscopically clean (NMR, absence of signals due to unreacted thiol or disulfide and acetate byproducts). Elemental analysis (Galbraith Laboratories, Knoxville, TN) of the dialyzed "3X, RT" tiopronin-MPC preparation (see Table 1) gave the following. Anal. Found: C, 10.39; H, 1.96; N, 2.99; S, 5.43; Au, 72.09. Calcd for C₄₂₅H₆₈₀O₂₅₅N₈₅S₈₅Au₂₀₁: C, 9.5; H, 1.27; N, 2.39; S, 5.09; Au, 74.19. Elemental analysis also shows that dialysis effectively removes salt impurities (Anal. Na, 472 ppm; Cl, 880 ppm), giving material $\geq 98.2\%$ in purity by mass. Longer dialysis times (168 h) produced materials of purity comparable to that found (Na, 500 ppm; Cl, 127 ppm) for alkanethiolate-MPCs prepared and purified as described earlier.^{4,5b}

Synthesis of Coenzyme A-Monolayer-Protected Clusters. In a typical reaction, 0.31 g of tetrachloroauric acid (0.84 mmol) and 0.116 g of coenzyme A (0.14 mmol) were codissolved

(14) Newkome, G. R.; Moorefield, C. N.; Vögtle, F. *Dendritic Molecules—Concepts, Synthesis, Prospectives*; VCH: New York, 1996.

(15) Christou, P. *Plant J.* **1992**, *2*, 275–281.

(16) Pietron, J. J.; Templeton, A. C.; Murray, R. W. Unpublished results.

(17) Denneberg, T.; Jeppson, J. O.; Stenberg, P. *Proc. Eur. Dial. Transplant Assoc.* **1983**, *20*, 427.

(18) Voet, D.; Voet, J. G. *Biochemistry*; Wiley: New York, 1990.

(19) *Handbook of Preparative Inorganic Chemistry*; Brauer, G., Ed.; AP: New York, 1965; p 1054. (b) Block, B. P. *Inorg. Synth.* **1953**, *4*, 14.

Table 1. Size and Composition Results for the Different Tiopronin–MPC Preparations

preparation conditions ^a	HRTEM ^b (dia, nm)	TGA, % organic ^c	atoms ^d (shape)	no. of surface atoms/% defects/area (nm ²)	% coverage/no. of chains ^e
3×, RT	1.8 ± 0.7	25.9	201 (TO)	128/47/15	66/85
1×, RT	2.2 ± 1.0	21.1	314 (TO ⁺)	174/41/19	58/101
1/6×, RT	3.1 ± 1.2	8	1289 (TO)	482/27/47	26/126
1/12×, RT	3.9 ± 1.7	8.4	2406 (TO) ^f	752/22/70	35/268
3×, 0 °C	2.0 ± 0.8	27	225 (TO ⁺)	140/43/15	59/82
3×, 65 °C	1.7 ± 0.6	21	201 (TO)	128/47/15	51/65

^a Code for preparation conditions: (x, y), where x is the ligand:AuCl₄⁻ molar ratio before reduction and y is the temperature at which the reduction was carried out. ^b High-resolution transmission electron microscopy results, average gold core diameter from analysis of histogram of at least two HRTEM images. ^c Thermogravimetric analysis for thermal loss of organic fraction of clusters. ^d For our analysis, we employ the shape model advocated by Whetten and used in previous studies.^{5b,12} TO = ideal truncoctahedron (all sides equal), TO⁺ = truncoctahedron in which (0 < n - m ≤ 4), where n is the number of atoms between (111) facets and m is the number of atoms between (111) and (100) facets. ^e As was done in a previous study of Au-based alkanethiolate–MPCs,^{5b} the average number of Au atoms in closed-shell, truncated octahedral cores¹² resulting from a particular cluster preparation can be represented by selecting the closed-shell “magic number” core size that has a combination of diameter and expected organic weight fraction that best matches the experimental data. With this core size, the number of surface atoms and protecting ligands can be established. ^f Owing to the presence of five discernible populations in the core size histogram, the atom and shape model here is derived from the average. The number of atoms and core shape model is more accurately described as a mixture of ~20% 314 (TO⁺), ~20% 807 (TO⁺), ~20% 1289 (TO), ~15% 4033 (TO), and ~8% 6266 (TO). The atom and shape components for the 3×, RT preparation used were as follows: ~30% 79 (TO⁺), ~25% 140 (TO⁺), ~15% 586 (TO), and 7% 807 (TO⁺).

in 35 mL of H₂O. NaBH₄ (0.38 g, 10 mmol) in 15 mL of H₂O was added to this rapidly stirred ruby red solution at room temperature; the solution immediately turned black and was stirred overnight, at which time the solvent was removed under vacuum. The CoA–MPCs were purified by dialysis as above for the tiopronin–MPCs except that the solution pH was not adjusted before dialysis.

Acid/Base Titration of Tiopronin–MPCs. In a typical titration, 50 mL of a stirred 2 mM aqueous solution (concentration in acid groups, assuming monolayer coverage in Table 1) of tiopronin–MPCs was titrated with 2 mM NaOH from a 50 mL analytical buret. The pH was followed from the ambient value (~3.7) to ca. 11 using a Corning 445 pH meter fitted with a standard glass/SCE combination electrode. The equivalence points were detected from pH vs V_{BASE} plots. Various concentrations of indifferent electrolyte (NaNO₃) were added to the titrated tiopronin–MPC solution.

Acid/Base Titration of CoA–MPCs. Titrations were as above except that 10–20 μL aliquots of 1 mM HCl were added to a stirred 10.4 μM aqueous CoA–MPC solution from a 100 μL Eppendorf automatic pipet.

Transmission Electron Microscopy (TEM). TEM samples were prepared by placing a single drop of a ca. 1 mg/mL aqueous MPC solution onto Formvar-coated (200–300 Å) copper grids (200 mesh), waiting 5 min, and removing excess solution by touching a small piece of filter paper to the edge of the grid. The grid was further dried under N₂ flow or in air for 5 or 30 min, respectively. Phase-contrast images of the MPCs were obtained with a side-entry Phillips CM12 electron microscope operating at 120 keV. Three typical regions of each sample were obtained at either 340000× or 430000×. Size distributions of the Au cores were obtained from at least two digitized photographic enlargements with Scion Image Beta Release 2 (available at www.scioncorp.com).

Thermogravimetric Analysis (TGA). Thermogravimetric analysis (TGA) was performed with a Seiko RTG 220 robotic TGA system, on 12–18 mg of dry, purified materials, under N₂ (flow rate of 50 mL/min), recording data from 25 to 600 °C at a heating rate of 20 °C/min. A brittle, gold-colored solid product resulted from the analysis that, following previous TGA work on alkanethiolate–MPCs,^{5b,20} was assumed to be elemental gold.

Spectroscopic Measurements. Proton NMR spectra were recorded at 200 MHz on a Bruker AC200 NMR spectrometer at room temperature in concentrated D₂O solutions (ca. 90 mg of MPC/mL). Typically, a line broadening factor of 1 Hz was used to improve NMR signal to noise (S/N) and a relaxation delay of 5 s was used to allow adequate signal decay between pulses.

UV–vis spectra (200–800 nm, 1 nm resolution) of aqueous ca. 1 mg/10 mL solutions in 1 cm quartz cells were recorded with an ATI UNICAM UV–vis spectrometer. Infrared spectra of solid MPC samples pressed into a KBr plate were recorded from 3800 to 500 cm⁻¹ with a Bio-Rad Model 6000 FTIR spectrometer.

Results and Discussion

Synthesis of Tiopronin–MPCs. Most previous monolayer-protected Au cluster syntheses^{4–13} invoke the (successful) tactic of using methylene-chain, hydrophobic ligands that, through tight and/or orderly packing, achieve excellent stabilization of nanometer-sized metal cores. There is no evidence extant whereby the bulky footprint of a thiolate ligand alone is sufficient to confer good Au MPC stabilization (especially as to isolation/redissolution). The steric bulk of the triphenylphosphine ligand was important in producing Au₅₅ clusters, an early example of MPCs,^{1,2} but this ligand proved not to be strongly stabilizing. We presently have in hand several examples of stabilization with molecules of significantly larger footprint than that of alkanethiolates, wherein the ligands are tiopronin and coenzyme A (the present study), ferrocenethiolate,²¹ and thiol-terminated polyethylene glycol.²² While any given example of a bulky thiolate may provide its own intraligand interactions that serve to add to the stability of the protecting monolayer, the diversity of the examples we have encountered strongly suggests that the mere steric bulk of protecting ligands can be a sufficient basis to prevent aggregating core–core interactions and, thus, for designing new types of MPCs. Besides ligand steric bulk and favorable intraligand interactions, both tiopronin and coenzyme A have ionizable groups which potentially form an electrostatic barrier to core–core coalescence.

Although there are multiple examples of colloids of Au (and CdS) which can be dispersed in water,^{2b–e} there are no examples extant in the literature of water-soluble gold nanoparticles which can be repeatedly isolated and redissolved. The synthesis of tiopronin–MPCs, illustrated schematically in Figure 1, involves several additional differences from the Brust reaction.⁴ (a) The reaction was executed in a methanol/acetic acid mixture rather than in toluene. In this solvent, codissolution of AuCl₄⁻ and

(20) Terrill, R. H.; Postlethwaite, T. A.; Chen, C.-H.; Poon, C.-D.; Terzis, A.; Chen, A.; Hutchison, J. E.; Clark, M. R.; Wignall, G.; Londono, J. D.; Superfine, R.; Falvo, M.; Johnson, C. S.; Samulski, E. T.; Murray, R. W. *J. Am. Chem. Soc.* **1995**, *117*, 12537–12548.

(21) Templeton, A. C.; Gross, S. M.; Murray, R. W. Manuscript in preparation.

(22) Wuelfing, W. P.; Gross, S. M.; Miles, D. T.; Murray, R. W., *J. Am. Chem. Soc.*, in press.

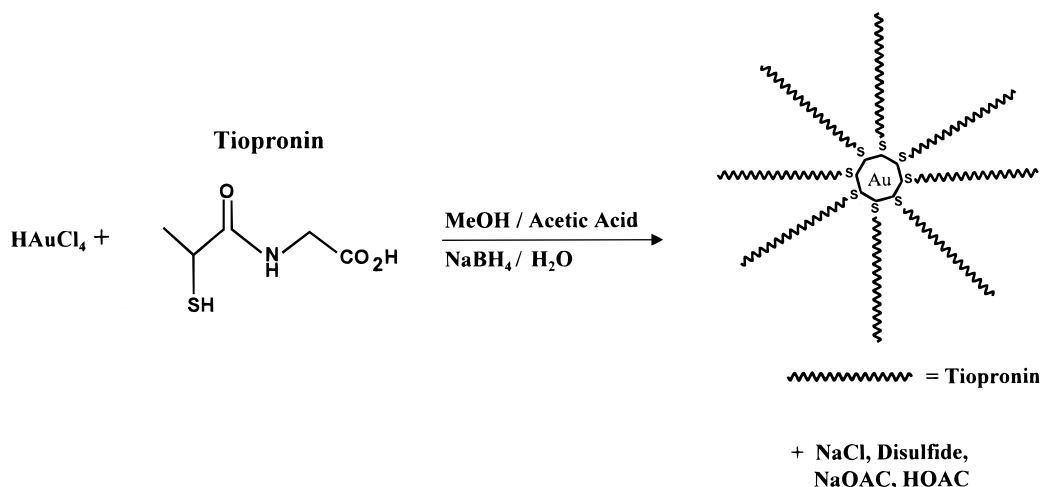


Figure 1. Schematic of synthesis of tiopronin monolayer-protected gold cluster compounds.

tiopronin (*N*-2-mercaptopropionylglycine) gave a stable ruby-red solution, indicating that the reduction of Au(III) by thiol (to form a colorless Au(I)–SR polymer), which typifies alkanethiol reactions in toluene in the Brust reaction,^{5b} does not occur in the present case (at nominal times). (b) Solution acidity was critical; in the absence of acetic acid, the nanoparticles formed upon BH_4^- addition immediately and irreversibly aggregated, and the reaction mixture pH rose to 10 (as opposed to the final pH of 5 with acetic acid present). These results suggest that nascent MPCs bearing deprotonated tiopronin are unstable in methanol. (c) MPCs produced by the BH_4^- reduction are insoluble in methanol (black suspension), but are water soluble. (d) Using water as the reaction medium leads to a water-insoluble product with comparatively large (ca. 16 nm) core. (e) The addition of NaBH_4 reductant solution was quite exothermic, producing a significant warming (24 to ca. 44 °C) of the reaction mixture. Since this thermal effect might influence the MPC product, reactions were also carried out with solutions that had been either warmed or precooled prior to reduction.^{5b} (f) The aqueous solubility of isolated tiopronin–MPCs is very specific; the products are not soluble in other polar solvents such as methanol, ethanol, DMF, acetone, or acetonitrile. (g) The tiopronin–MPC is a finely divided black powder and lacks the waxy consistency typical of long-chain alkanethiolate–MPCs.^{4,5b}

The tiopronin–MPCs were purified of water-soluble byproducts (Figure 1) and unreacted starting materials by dialysis, following which ^1H NMR analysis showed that they were free of monomer, disulfides, and acetates. Elemental analysis showed salt residues (NaCl) to be quite low (see Experimental Section). The salt residues after 72 h of dialysis were about twice that seen for Au-based alkanethiolate–MPCs that had been purified by precipitation and filtration but after 168 h of dialysis were about the same.

High-Resolution Transmission Electron Microscopy (HRTEM). Electron microscopy has provided important information about alkanethiolate monolayer-protected gold clusters. For example, HRTEM and laser desorption/ionization (LDI) mass spectrometric data were combined with theoretical calculations in a proposal¹² that the most probable gold core shapes in closed-shell alkanethiolate–MPCs are truncated octahedra. Other HRTEM images have illustrated patterned self-assembly of gold-based alkanethiolate–MPCs^{23,24} and spacings be-

tween cores that correlate with the chain lengths in the protecting alkanethiolate monolayers.^{5b,24e}

In this study, HRTEM was used to assess the dispersity of the tiopronin–MPC core sizes and to follow the dependency of average core size on the mole ratio of tiopronin and AuCl_4^- used in the cluster synthesis (see Table 1, footnote *a*, for coding of reaction conditions). Figure 2 gives illustrative HRTEM images and core size histograms for the most thiol-rich ($3\times$, RT) and poor ($1/12\times$, RT) preparation. (See Supporting Information for others.)

The Table 1 results for average core size show that, like alkanethiolate–MPCs, thiol-rich reactions yield smaller Au cores (than thiol-deficient conditions). Interestingly, the tiopronin–MPC core sizes obtained under thiol-deficient conditions (tiopronin: AuCl_4^- ratio < 1:1) are smaller than those of alkanethiolate–MPCs obtained^{5b} using the same thiol/ AuCl_4^- reaction ratio; the difference for the $1/12\times$, RT preparation is a full 1.3 nm smaller average core diameter.^{5b} (Analogous results are obtained in other syntheses employing thiols with sterically bulky substituents.^{21,22,25}) The relative rates of core passivation and growth may tend to be enhanced by sterically bulky monolayer ligands, but of course these rates may be influenced by other factors including the different reaction solvents (methanol for tiopronin, toluene for alkanethiols).

The Figure 2 HRTEM images reveal substantial dispersity in the tiopronin–MPC Au core sizes and the presence of uneven distributions. The size distributions in all of the $3\times$ preparations (RT in Figure 2a, 0 and 65 °C in Supporting Information) are biased toward smaller core sizes. Thus, while the average core diameter in the $3\times$, RT preparation (Table 1) is 1.8 ± 0.7 nm, ~64% of the population has an average 1.5 ± 0.6 nm diameter. The $3\times$, 65 °C preparation is even more dominated by smaller cores, having ~75% of its population centered on 1.5 ± 0.5 nm, as is the $1\times$, RT preparation with ~70% of the population lying at 1.9 ± 0.6 nm diameter.

(24) Ohara, P. C.; Leff, D. V.; Heath, J. R.; Gelbart, W. M. *Phys. Rev. Lett.* **1995**, *75*, 3466–3469. (b) Brust, M.; Bethell, D.; Schiffrin, D. J.; Kiely, C. J. *Adv. Mater.* **1995**, *7*, 795–797. (c) Fink, J.; Kiely, C. J.; Bethell, D.; Schiffrin, D. J. *Chem. Mater.* **1998**, *10*, 922–926. (d) Murthy, S.; Wang, Z. L.; Whetten, R. L. *Philos. Mag. Lett.* **1997**, *75*, 321–327. (e) Giersig, M.; Mulvaney, P. *Langmuir* **1993**, *9*, 3408–3413.

(25) Efforts to further probe this effect with a thiol at a tertiary site indeed produced smaller particles, but the materials were insoluble in water. A synthesis performed with *D*-penicillamine (*D*-[–]-2-amino-3-mercaptomethylbutanoic acid) using the same conditions as that reported here for tiopronin gave clusters (HRTEM analysis) with an average core size of ~1.2 nm.

(23) Hostetler, M. J.; Murray, R. W. Unpublished results.

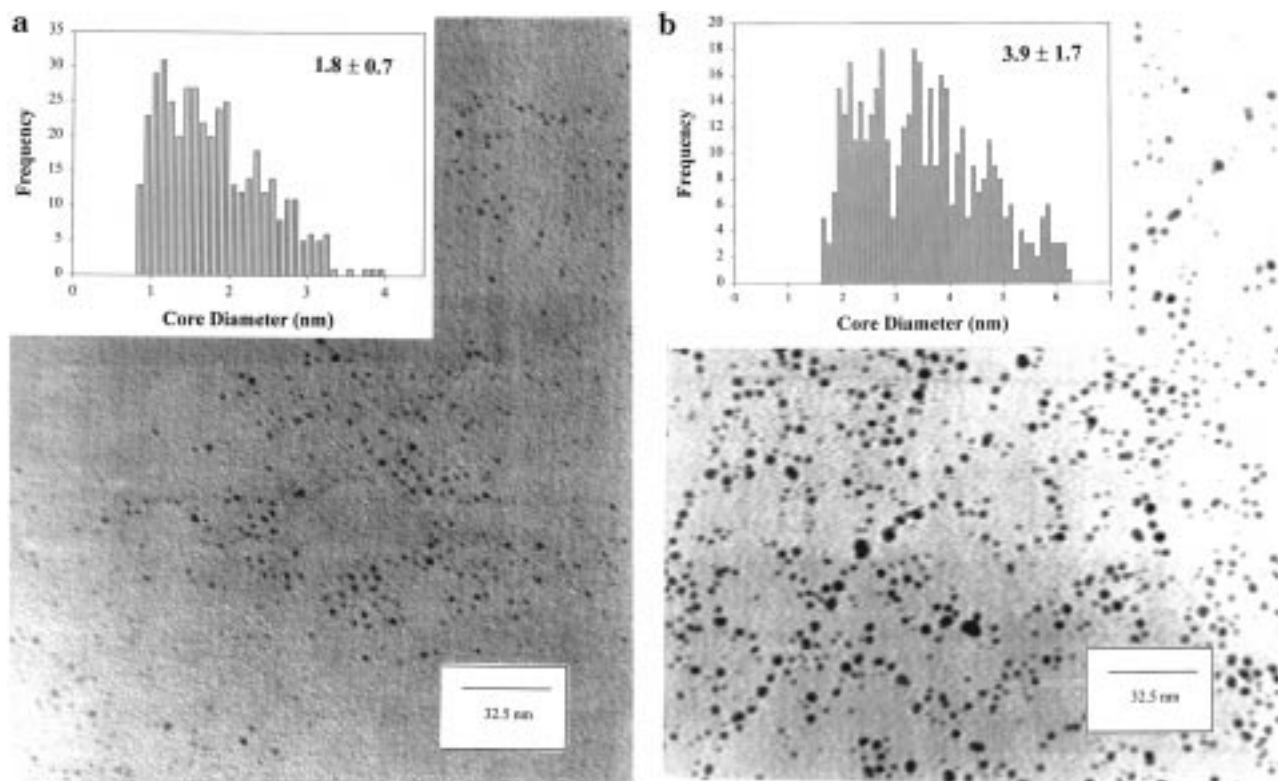


Figure 2. Transmission electron micrographs and core size histograms (insets) of tiopronin-MPCs: (a) ($3\times$, RT), (b) ($1/12\times$, RT). Average particle diameters are noted in the insets. TEM micrographs and histograms of other preparations are given in Supporting Information.

The HRTEM histograms also exhibit indistinct modalities in the core populations (Figure 2a inset); such modalities can be interpreted as reflecting preferences for closed-shell (“magic number”) truncated octahedral core structures.¹² The histogram modalities are more obvious for the thiol-deficient preparations, which are also overall more disperse as might be expected since the ideal simultaneous nucleation that leads to synchronization of growth and passivation is less likely under thiol-deficient conditions. The histogram of the $1/12\times$, RT preparation (Figure 2b inset) exhibits ca. equal populations centered at 2.1, 2.7, and 3.3 nm that comprise $\sim 70\%$ of the overall population, with two smaller populations at 4.8 nm ($\sim 15\%$) and 6 nm ($\sim 8\%$). The histogram for the $1/6\times$, RT preparation displays a core size population ($\sim 30\%$) centered at 2.8 nm with smaller peaks in the histogram at 1.9 nm ($\sim 15\%$), 3.3 nm ($\sim 20\%$), and 3.7 nm ($\sim 15\%$). While the HRTEM data are consistent with preferred core sizes as anticipated from prior work,^{5b,12} the resolution of the images is insufficient to rule out clusters with nonpreferred core shapes or non-closed-shell core structures. The MPC synthesis is, after all, a nucleation-growth-passivation reaction, and some kinetic control of the MPC cores formed should not be surprising.

Thermogravimetric Analysis (TGA). Previous results^{5b} have shown that MPCs decompose thermally by loss of the monolayer as (primarily) volatile disulfides, leaving an elemental gold residue. Thermogravimetric analysis (TGA) is thus a convenient route to determine the organic weight fraction of MPCs. TGA data for tiopronin-MPCs are also given in Table 1. The organic weight fraction decreases sharply with increasing core size, as anticipated from geometrical considerations. As was done in a previous study of Au-based alkanethiolate-MPCs,^{5b} the average number of Au atoms in closed-shell, truncated octahedral cores¹² resulting from a particular

cluster preparation can be represented by selecting the closed-shell “magic number” core size that has a combination of diameter and expected organic weight fraction that best matches the experimental data. These average representations are given in Table 1, along with the corresponding numbers of Au core surface atoms and the percentages of them that lie on edges and vertexes (% defects) and other parameters calculated as described previously for alkanethiolate-MPCs.^{5b}

The monolayer coverage (ligands/surface atoms) in Table 1 increases for the smaller core MPCs owing primarily to the larger fraction of “defect” (edges and vertexes) Au sites and attendant sharper radii of curvature, which is consistent with alkanethiolate-MPCs.^{5b} A larger effective packing density for ligands on smaller-core MPCs is also inferred from the ligand footprint size, which is 0.18 vs 0.26 nm²/ligand for the $3\times$, RT vs $1/12\times$, RT preparations, respectively. For comparison, model calculations using commercial software (Hyperchem, no nearest-neighbor interactions included) to generate an energy-minimized tiopronin monomer conformation give a cross-sectional area of ca. 0.25 nm². This is $\sim 20\%$ larger than the reported footprint of straight-chain alkanethiolates on gold, which is 0.21 nm².²⁶ That the experimental tiopronin footprints are smaller than the calculated value must reflect how the strongly curved MPC core surface allows a larger effective packing density of ligands.

The experimental footprints are crude values, however, since they ignore the core size averaging in the Table 1 results. A better estimate can be made using the multimodal distributions in the experimental core size histograms. With estimates of the fractional populations in the histograms of each core size (see above), and identi-

(26) Sellars, H.; Ulman, A.; Schnidman, Y.; Eilers, J. E. *J. Am. Chem. Soc.* **1993**, *115*, 9389–9401.

fication of the number of Au atoms appropriate for each core size (see Table 1 footnotes), the total core area was evaluated as a weighted average of areas of the different core size populations. This calculation²⁷ gave even smaller experimental footprints—0.14 and 0.19 nm²/ligand for the 3 \times , RT and 1/12 \times , RT preparations, respectively—and again show a larger effective packing density for the smaller-core MPC.

Temperature effects on the cluster synthesis were relatively modest. The clusters produced by addition of reductant to reaction mixtures at room temperature or precooled to 0 °C were not very different in average core size or ligand coverage (Table 1). On the other hand, warming the reaction mixture to 65 °C (boiling methanol) prior to reductant addition produced MPCs with slightly smaller (both average and based on population distribution) cores, yet with a substantially lower ligand coverage (51%). These clusters can be inferred to have a lower ligand packing density, i.e., a ligand coverage less complete than on those produced at lower temperatures. This temperature effect is analogous to that experienced with alkanethiolate-MPCs.^{5b}

The thermal decomposition of all the tiopronin-MPCs occurred in single, well-defined steps that begin at \sim 231 °C and are completed after a further increase of ca. 100 °C. The analogous decomposition temperatures for Au-based alkanethiolate-MPCs change roughly linearly with chain length (ca. 40 °C/C4 unit).^{5b,20} Tiopronin has a chain length analogous to that of pentanethiol, for which the decomposition temperature is \sim 200 °C. The observed tiopronin-MPC thermal decomposition occurs more closely to that of octanethiolate-MPCs (230 °C). These comparisons show that tiopronin-MPCs are thermally stabilized relative to alkanethiolate-MPCs, which may arise from the stabilizing effect of intercluster hydrogen bonding between ligands on adjacent clusters (vide infra) and/or the different nature of the disulfide evolved.

¹H NMR Spectroscopy. Spectra of D₂O solutions of tiopronin-MPCs are given in Figure 3. The several factors that contribute to the characteristic broadening of resonances in MPC spectra (relative to monomer ligand) have been discussed in detail elsewhere.^{5b,20,28} The general increase in broadening with tiopronin-MPC core size is qualitatively consistent with spin-spin relaxation (T_2); i.e., rotational motions of the larger, 3.9 nm average core size MPCs (Figure 3d), are significantly slower than those of the smallest, 1.8 nm average core size (Figure 3a). Further broadening is caused by the gradient of packing density along the ligand chain, presumably causing the CH₃-resonance ($\delta = 1.2$ –1.9) to be broader than that ($\delta = 3.7$ –4.0) of the methylene protons located two atoms further away from the core. An interesting spectral characteristic is that the methine and methyl peaks are not broadened as severely as might be expected considering the behavior of alkanethiolate-MPCs.^{5b,20,28} The unexpected narrowness of the methine peak gives rise to the notion that the methine proton site is sterically blocked so that its relaxation decay is inconsistent with "solid-state" packing density behavior. Stated differently, the methine proton is attached to a secondary carbon site that forces a local packing density lower than that at the same location in typical alkanethiolate MPC monolayers.

A distribution of chemical shifts^{5b,28} can also lead to

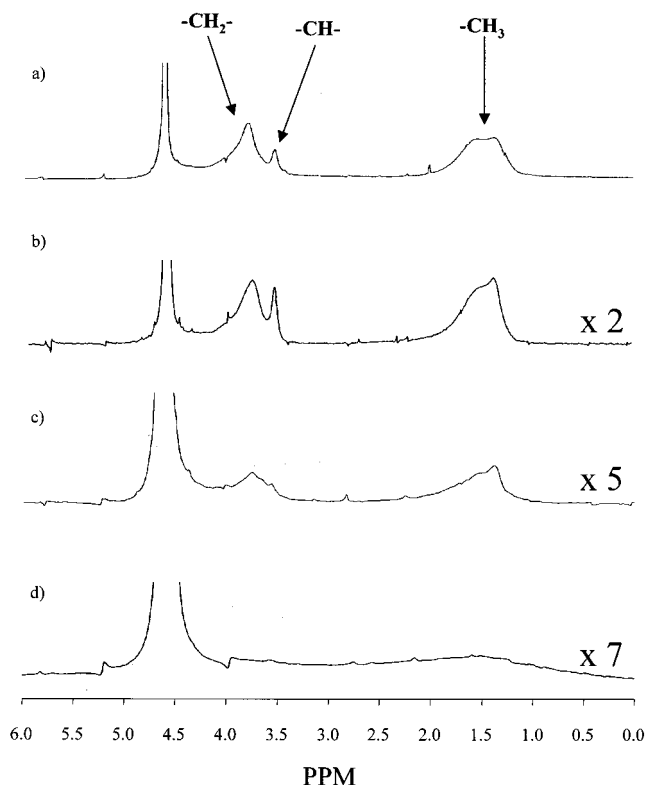


Figure 3. ¹H NMR spectra of D₂O solutions of tiopronin-MPCs. Each spectrum was Fourier transformed using a line broadening factor of 1 Hz. Relative integrated intensities of methylene:methine:methyl resonances are, respectively: (a) 3 \times , RT preparation (average diameter 1.8 nm), 2.4:0.4:3 (b) 1 \times , RT preparation (average diameter 2.2 nm), 2.1:0.4:3, (c) 1/6 \times , RT preparation (average diameter 3.1 nm), 2:0.4:3, and (d) 1/12 \times , RT preparation (average diameter 3.9 nm), integrations could not be measured. Spectra are shown at different magnifications in order to facilitate comparison.

peak broadening in MPC spectra; chemical shift differences can arise from the intrinsic heterogeneity of the (nonspherical) core surface and the consequent differences between ligand binding sites (i.e., edges, vertices, terraces). Effects of this kind are present in the tiopronin-MPC spectra. The 40 Hz separation between the two peaks for the methyl group (at $\delta = 1.3$ and 1.6 ppm, Figure 3a) is too large²⁹ to arise from spin-spin splitting (only 10 Hz in the monomer ligand), and there is no comparable quartet splitting of the methine peak. Additionally, in Figure 3a–c, the upfield member of the two methyl peaks is more narrow than the downfield member, meaning that the methyl groups are subject to a differential broadening effect as well as having different chemical shifts. Further, there may also be two kinds of methine protons; the relative integrated peak intensities in Figure 3a for the methylene ($\delta = 3.7$ –4.0 ppm), methine ($\delta = 3.6$ ppm), and methyl ($\delta = 1.3$ and 1.6 ppm) groups, ideally 2:1:3, are instead 2.4:0.4:3. The larger methylene intensity and smaller methine intensity suggest that a second methine component, lying at ca. 0.2 ppm downfield, may be buried under the methylene peak. The different kinds of methyl and methine protons could arise from differences in the tiopronin binding sites on the Au core³⁰ (such as defect vs

(29) Friebolin, H. *Basic One- and Two-Dimensional NMR Spectroscopy*; VCH: New York, 1993.

(30) Additional evidence comes from experiments conducted with Au/Pd alloys wherein methylene resonances originating from two different cluster surface sites are postulated. Hostetler, M. J.; Zhong, C.-J.; Yen, B. K. H.; Anderegg, J.; Gross, S. M.; Evans, N. D.; Porter, M. D.; Murray, R. W. *J. Am. Chem. Soc.* **1998**, *120*, 9396–9397.

(27) The 3 \times , RT and 1/12 \times , RT preparations were modeled using the values of footnote e in Table 1 and gave core areas of 12.1 nm² to 51 nm², respectively. Modeling the core as a sphere and calculating the average area from all histogram data give numbers that support the same trend.

(28) Badia, A.; Gao, W.; Singh, S.; Demers, L.; Cuccia, L.; Reven, L. *Langmuir* **1996**, *12*, 1262–1269.

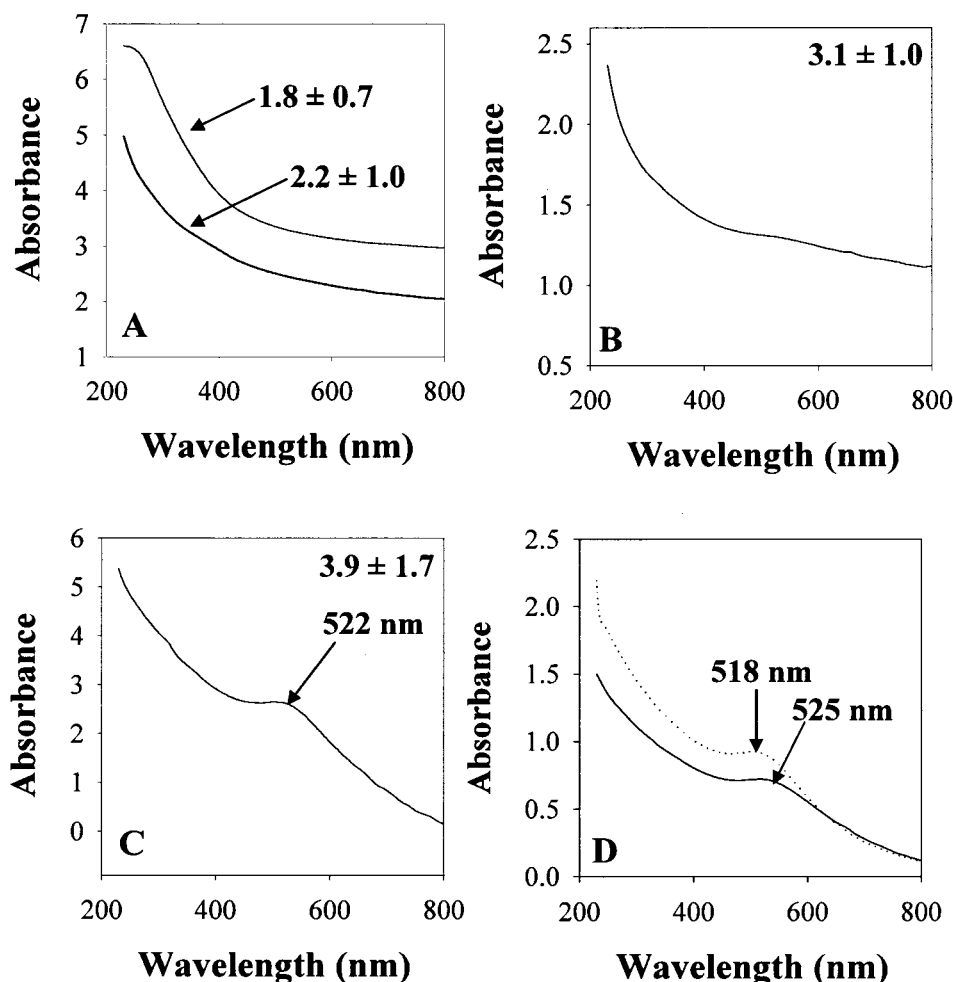


Figure 4. UV-vis spectra (H_2O) of tiopronin-MPCs: (A) $3\times$, RT preparation, 1.8 ± 0.7 nm average core diameter, 5.6×10^{-4} M (based on MW = 53 kD); $1\times$, RT preparation, 2.2 ± 1.0 nm average core diameter, 2.3×10^{-6} M (based on MW = 78 kD); (B) $1/6\times$, RT preparation, 3.1 ± 1.0 nm average core diameter, 9×10^{-7} M (based on MW = 274 kD); (C) $1/12\times$, RT preparation, 3.9 ± 1.7 nm average core diameter, 1.6×10^{-7} M (based on MW = 520 kD); (D) $1/12\times$, RT preparation, 3×10^{-7} M, solution pH adjusted to 1 (—) and 12 (---).

terrace sites). Another possibility is conformational differences, owing to chain packing or binding site, which force the methyl groups to lie at varying distances from the gold core and (from differences in magnetic susceptibilities) experience different magnetic fields.²⁰

Finally, also of note is a small peak which appears superimposed on the methylene resonance in Figure 3c. It is possible that this peak is the second methine peak, and its appearance in this spectra can be attributed to the disproportionate nature of the surface site populations between the three samples.

UV-vis Spectroscopy. Electronic spectra of alkanethiolate-MPCs have been the subject of several recent papers.^{5b,31} Like these materials, the UV-vis spectra of aqueous tiopronin-MPC solutions (Figure 4) depend strongly on core size. The UV absorbance of the smallest clusters decays in an approximately exponential fashion into the visible, with no detectable surface plasmon band (SP band, Figure 4a).^{5b} The SP band is more detectable for the larger clusters (Figure 4b,c) and most easily so for the largest core MPC ($\lambda_{\text{MAX}} = 522$ nm), but the SP band

intensity is lower for the tiopronin-MPCs than for the alkanethiolate-MPCs. Whether this effect arises from differences in dielectric properties of alkanethiolate vs tiopronin monolayers or from some other factor is unclear.³²

The SP band also depends on the solution pH, as shown in Figure 4d, where the pH of the neutral (pH = 7) solution of $1/12\times$, RT tiopronin-MPCs in Figure 4c has been adjusted to pH 1 (solid line) and pH 12 (dashed line). An accompanying shift is observed (values shown on figure). Control experiments³³ show that the resulting shift in λ_{MAX} of the SP band (to lower energy at lowered pH) is reversible and not due to base-catalyzed amide hydrolysis. pH-induced MPC aggregation would be expected to cause larger wavelength shifts. Again, it is most likely that the shift arises from a difference between the effective dielectric properties of the monolayer in protonated vs anionic states.³⁴ Additional evidence is found in the UV-vis spectra of the CoA-MPCs (vide infra).

Infrared Spectroscopy. Leveraged by the consider-

(31) See, for example: (a) Schaaf, T. G.; Shafiqullin, M. N.; Khoury, J. T.; Vezmar, I.; Whetten, R. L.; Cullen, W. G.; First, P. N.; Gutiérrez-Wing, C.; Ascensio, J.; Yose-Yacamm, M. J. *J. Phys. Chem. B* **1997**, *101*, 7885–7891. (b) Vezmar, I.; Alvarez, M. M.; Khoury, J. T.; Salisbury, B. E.; Whetten, R. L. *Z. Phys. D* **1997**, *40*, 147. (c) Underwood, S.; Mulvaney, P. *Langmuir* **1994**, *10*, 3427–3430. (d) Mulvaney, P. *Langmuir* **1996**, *12*, 788–800.

(32) Person, B. N. *J. Surf. Sci.* **1993**, *281*, 153–162.

(33) Following adjusting the pH to 12 and recording the UV-vis spectra (Figure 4d, solid line), the pH was readjusted to 1 and a spectrum identical to that shown for the pH = 1 sample (Figure 4d, dotted line) was reproduced. (b) A control experiment on the pH stability of the free ligand was conducted by adjusting a 25 mL aqueous solution containing 100 mg of tiopronin to pH 12. Following solvent removal, the ^1H NMR spectrum is consistent with the amide bond remaining intact.

Table 2. Selected IR Band Assignments and Positions for Tiopronin and Tiopronin–Monolayer Protected Clusters^a

tiopronin (monomer) ^b	3×, RT ^c (1.8 ± 0.7) ^d	1×, RT (2.2 ± 1.0)	1/6× (3.1 ± 1.2)	1/12×, RT (3.9 ± 1.7)	assignment
1557, s ^e	1529, s	1526, s	1525, s	1517, s	amide II
1622, s	1640, s	1638, s	1639, s	1631, s	amide I
1754, s	1727, s	1727, s	1722, s	1722, s	C=O stretch
2565, m					S–H stretch
3091, s	3062, br	3081, br			amide B
3316, s	3394, br	3422, br	3438, br	3435, br	amide A

^a Only those bands of significant intensity and relevance to confirming the presence or absence of hydrogen bonding in these materials are considered here. ^b Data for ligand unattached to gold cluster. ^c Code for preparation conditions for all samples: (x, y), where x is the ligand:AuCl₄⁻ molar ratio before reduction and y is the temperature at which the reduction was carried out. ^d Average core size with standard deviation from core size histograms. ^e Data in table refer to peak position (in cm⁻¹) and intensity, where s denotes strong, m denotes medium, and br denotes broad.

able literature³⁵ of self-assembled alkanethiolate monolayers on flat Au(111), vibrational spectroscopy of alkanethiolate–MPCs has provided valuable insight into the conformational ordering of their monolayers.^{5b,36} Considerable evidence for hydrogen bonding interactions in amide-containing thiolate monolayers on flat gold surfaces has also been given in several recent papers.³⁷ Hydrogen bonding interactions in the tiopronin–MPCs were viewed as likely; a more complex question is that hydrogen bonding might occur in several different ways in tiopronin–MPCs: (a) between amides of ligands on the same cluster (*parallel*, or *intra-MPC*) and (b) between amides of ligands on different clusters (*antiparallel*, *inter-MPC*), and similarly (c) between carboxylic acid groups of ligands on the same cluster and (d) on different clusters.

IR spectra of the tiopronin monomer and of the 3×, RT cluster preparation are given in Figure 5; key positions and band assignments are summarized in Table 2. Amide A bands (~3300 cm⁻¹) correspond to N–H stretching vibrations while the amide B band (~3100 cm⁻¹) is a Fermi resonance-enhanced overtone of the amide II band.³⁸ The amide carbonyl is usually trans to the N–H group and its stretching band (amide I) normally appears at ~1630–1680 cm⁻¹. The amide II band (~1500–1600 cm⁻¹) arises from N–H and C–N torsional motions; other torsional motions can yield the very weak amide III band at ~1250–1310 cm⁻¹. The presence and location of the various amide bands are of particular interest in determining the nature of hydrogen-bonding interactions within the tiopronin–MPC ligand environment.

Like amide-containing two-dimensional self-assembled monolayers (2D-SAMs) described in the literature,³⁷ the N–H stretching vibrations (amide A) of solid tiopronin–MPC samples (Figure 5b, ~3394 cm⁻¹) exhibit strong evidence for hydrogen bonding interactions. Unassociated amide A bands are relatively sharp (i.e., the monomer spectrum, Figure 5a), while those involved in hydrogen

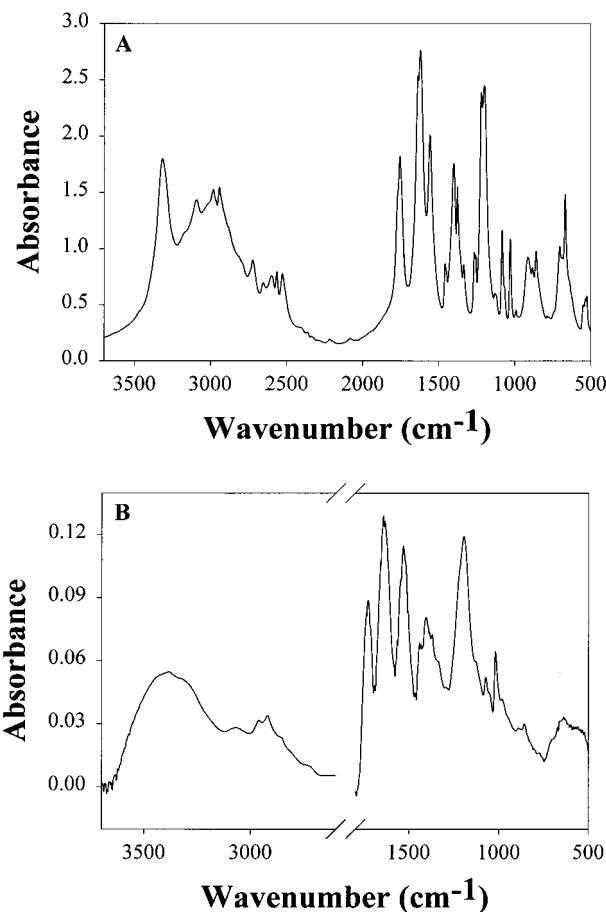


Figure 5. Transmission FTIR spectra of (A) tiopronin monomer and (B) 3×, RT tiopronin–MPC (average diameter 1.8 nm). All spectra were acquired in the form of KBr plates, and intensities of the bands are uncorrected for sample quantity.

bonding associations experience substantial broadening, which is seen in Figure 5b. The N–H stretches for the different tiopronin–MPCs lie at somewhat higher energy than the monomer (80–100 cm⁻¹). The lower energy of the tiopronin–MPC amide II band as compared to the monomer (1557 cm⁻¹) provides evidence that the hydrogen bonding is *antiparallel*, *intercluster*, which could transpire through interdigitation of ligands or ligand bundles on adjacent cluster molecules as postulated previously for alkanethiolate–MPCs.^{5b,19} The 1557 cm⁻¹ position of the amide II band for the tiopronin monomer is very close to that reported by Cha et al.³⁹ (1550 cm⁻¹) for polyglycine II in a parallel configuration and to other reports on self-assembled monolayers.^{37b–e} The amide II band positions

(34) Additional experiments and modeling are currently being pursued to understand changes of the surface plasmon band maximum with size and pH.

(35) Nuzzo, R. G.; Fusco, F. A.; Allara, D. L. *J. Am. Chem. Soc.* **1987**, *109*, 2358–2368. (b) Porter, M. D.; Bright, T. B.; Allara, D. L.; Chidsey, C. E. D. *J. Am. Chem. Soc.* **1987**, *109*, 3559–3568. (c) Bryant, M. A.; Pemberton, J. E. *J. Am. Chem. Soc.* **1991**, *113*, 8284–8293.

(36) Hostetler, M. J.; Stokes, J. J.; Murray, R. W. *Langmuir* **1996**, *12*, 3604–3612.

(37) Nuzzo, R. G.; Dubois, L. H.; Allara, D. L. *J. Am. Chem. Soc.* **1990**, *112*, 558–569. (b) Lenk, T. J.; Hallmark, V. M.; Hoffman, C. L.; Rabolt, J. F.; Castner, D. G.; Erdelen, C.; Ringsdorf, H. *Langmuir* **1994**, *10*, 4610–4617. (c) Tam-Chang, S.-W.; Biebuyck, H. A.; Whiteside, G. M.; Jeon, N.; Nuzzo, R. G. *Langmuir* **1995**, *11*, 4371–4382. (d) Clegg, R. S.; Hutchison, J. E. *Langmuir* **1996**, *12*, 5239–5243. (e) Sabapathy, R. C.; Bhattacharyya, S.; Leavy, M. C.; Cleland, W. E.; Hussey, C. L. *Langmuir* **1998**, *14*, 124–136. (f) Clegg, R. S.; Reed, S. M.; Hutchison, J. E. *J. Am. Chem. Soc.* **1998**, *120*, 2486–2487.

(38) See discussion and references cited in Bellamy, L. J. *The Infrared Spectra of Complex Molecules*; Chapman and Hall: New York, Volume 1.

(39) Cha, X.; Ariga, K.; Kunitake, T. *Bull. Chem. Soc. Jpn.* **1996**, *69*, 163–168.

for the tiopronin-MPCs are, in turn, close to the anti-parallel hydrogen bonding amide II reported for polyglycine I (1517 cm^{-1}).³⁸ Tam-Chang et al. have described^{37c} the geometrical requirements for strong hydrogen bonding within a self-assembled monolayer on gold. These requirements should be more difficult to meet on the highly curved MPC core surface, relative to a 2D-SAM, so we postulate that the hydrogen bonding is more likely by interdigitation and are *intercluster* rather than *intracluster* interactions.

The amide I band position (Table 2, $\sim 1639\text{ cm}^{-1}$) in tiopronin-MPCs is consistent with that of amide-containing SAMs³⁷ and lies at higher energy than that of the tiopronin monomer (1622 cm^{-1}). This contrast implies some differences between hydrogen bonding in the monomer versus the MPC, an interpretation based largely on literature precedent.³⁸

The carboxylic acid grouping on the tiopronin ligand is, of course, also a potential locus of hydrogen bonding. In the monomer, the acid carbonyl stretch position is consistent with that for a non-hydrogen-bonding group,^{37a,38} while that of the tiopronin-MPCs is shifted to lower energy. Nuzzo and co-workers^{37a} have interpreted such shifts in 2D-SAMs as reflecting weak hydrogen bonding between terminal carboxylic acid groups. This is consistent with the hydrogen bonding suggested in the carboxylic acid O-H stretch³⁸ by the broadened feature at $\sim 2700\text{--}2900\text{ cm}^{-1}$ (Figure 5a,b). Carboxylic acid head-to-head dimer formation, a manifestation of stonger hydrogen bonding, typically produces bands at $\sim 1699\text{ cm}^{-1}$,³⁸ which are not seen in Figure 5b. The absence of this form of hydrogen bonding (*inter-* or *intracluster*) can be rationalized by its competition with the apparent interdigitation involved with amide hydrogen bonding.

Indirect evidence for *intercluster* hydrogen bonding is derived from the solubility behavior of tiopronin-MPCs, which, while soluble in water, are only very slightly soluble in other high-polarity solvents (methanol, ethanol, acetone, DMF, or acetonitrile). This behavior suggests that highly favorable intercluster interactions (e.g., hydrogen bonding) must be overcome in order to solubilize the clusters, and the capacity of water in regard to hydrogen bonding solvation is effective in that regard.

Besides the bands relevant to determining hydrogen bonding interactions, we note the absence of a SH stretch at $\sim 2565\text{ cm}^{-1}$ in the infrared spectra of tiopronin-MPCs. These data, along with ¹H NMR, are consistent with earlier observations^{5b,36} for alkanethiolate-MPCs, and confirm that the -SH proton is lost in the reactions that lead to formation of the tiopronin monolayer-protected Au core.

The combined vibrational spectral features of tiopronin-MPCs show (a) that hydrogen bonding is an important force in interactions between clusters and is more prominent in the amide than in the carboxylic acid groups and (b) that chain or chain-bundle interdigitation probably occurs between adjacent clusters (consistent with TEM images of alkanethiolate-MPCs where the cluster core-core spacing approximately equals one chain length). Last, it should be emphasized that the above observations are on solid state MPC samples; hydrogen-bonding interactions in aqueous solutions of tiopronin-MPCs are likely to be quite different and probably weaker and are not considered in this study.

Neutralization of Tiopronin-MPCs: Acid/Base Titrations. Some details of the acid-base behavior of carboxylic acid groups in self-assembled monolayers on

flat Au(111) surfaces have been reported,⁴⁰ but there are no analogous studies of MPC clusters. The large available quantities of -CO₂H groups in tiopronin-MPC solutions allow a direct approach to study of their acidity, by titrating them with strong base.

Figure 6 summarizes titration curves of the free tiopronin ligand (6a, —) and of 3 \times , RT (6a, \cdots) and ¹/₁₂ \times , RT (6c, —) tiopronin-MPC preparations, along with values of the apparent pK_A calculated for various stages of neutralization (insets, same legend). The tiopronin monomer (Figure 6a, —) exhibits a sharp equivalence point and a pK_A (3.51 ± 0.33) that varies to a minor extent at different stages of neutralization (see inset). In contrast, the titration curve (Figure 6a, \cdots) for 3 \times , RT (1.8 nm average) tiopronin-MPCs is substantially smeared relative to that of the free ligand, and the apparent pK_A displays an appreciable lessening of MPC acidity as the cluster is neutralized. The average pK_A is almost 2 units higher (5.56 ± 0.53) than the monomer. These effects are undoubtedly electrostatic in nature; the fully neutralized (average) tiopronin-MPC molecule carries ca. 85 negatively charged carboxylate groups. An acidity change may also result from attachment of the ligand to the gold cluster surface. The electrostatic effect was probed by adding various concentrations of indifferent electrolyte (NaNO₃) to the titration medium (Figure 6b). NaNO₃ (20 mM) added electrolyte (6b, —) lowers the average pK_A by 0.80 unit (4.77 ± 0.41), relative to the result with no added electrolyte, while 1 M NaNO₃ (\cdots) lowers the average pK_A by 1.5 units (3.95 ± 0.27). Clearly, the availability of a large concentration of cation image charges in the solution lowers the apparent pK_A of the carboxylic acid groups by lowering the thermodynamic cost of generating negative sites as the cluster is neutralized. However, while the titration break becomes sharper and the drift in apparent pK_A is lessened in Figure 6b, there are still changes in the apparent pK_A as neutralization proceeds (see inset), even in 1 M electrolyte, and the apparent pK_A remains larger than that of the free ligand. This was also seen in a titration of a larger average core size (3.9 nm) tiopronin-MPC, such as seen in Figure 6c. With 1 M NaNO₃ added, the observed average pK_A (4.1 ± 0.42) is similar to the smaller clusters titrated under the same conditions (Figure 6b). The packing density of the tiopronin ligands is so large that even large electrolyte concentrations are insufficient to screen all of the charge repulsive interactions.

The acidity effects in the tiopronin-MPC titrations are qualitatively analogous to titration of any polyprotic acid, including a polymeric polyprotic acid. Whereas a linear polymer containing multiple acid groups becomes elongated to minimize charge repulsion, hyperbranched polymeric systems such as dendrimers cannot and, thus such as tiopronin-MPCs, experience larger effects.⁴¹

Coenzyme A Monolayer-Protected Clusters (CoA-MPCs). Coenzyme A is an important enzyme cofactor involved in acyl transfer in the citric acid cycle. CoA-terminated gold clusters are of interest in producing designed MPCs that utilize this enzymatic pathway.

The synthesis of CoA-MPCs differs slightly from the tiopronin-MPC synthesis in that the CoASH/AuCl₄⁻ mixture was reduced with NaBH₄ in water as solvent and

(40) Hu, K.; Bard, A. J. *Langmuir* **1997**, *13*, 5114–5119. (b) Jordan, C. E.; Corn, R. M. *Anal. Chem.* **1997**, *69*, 1449–1456. (c) Vezenov, D. V.; Noy, A.; Rozsnyai, L. F.; Lieber, C. M. *J. Am. Chem. Soc.* **1997**, *119*, 2006–2015. (d) Bain, C. D.; Whitesides, G. M. *Langmuir* **1989**, *5*, 1370–1378. (e) Bryant, M. A.; Crooks, R. M. *Langmuir* **1993**, *9*, 385–387. (f) Godinez, L. A.; Castro, R.; Kaifer, A. E. *Langmuir* **1996**, *12*, 5087–5092.

(41) Van Duijvenbode, R. C.; Borkovec, M.; Koper, J. M. *Polymer* **1998**, *39*, 2657–2664.

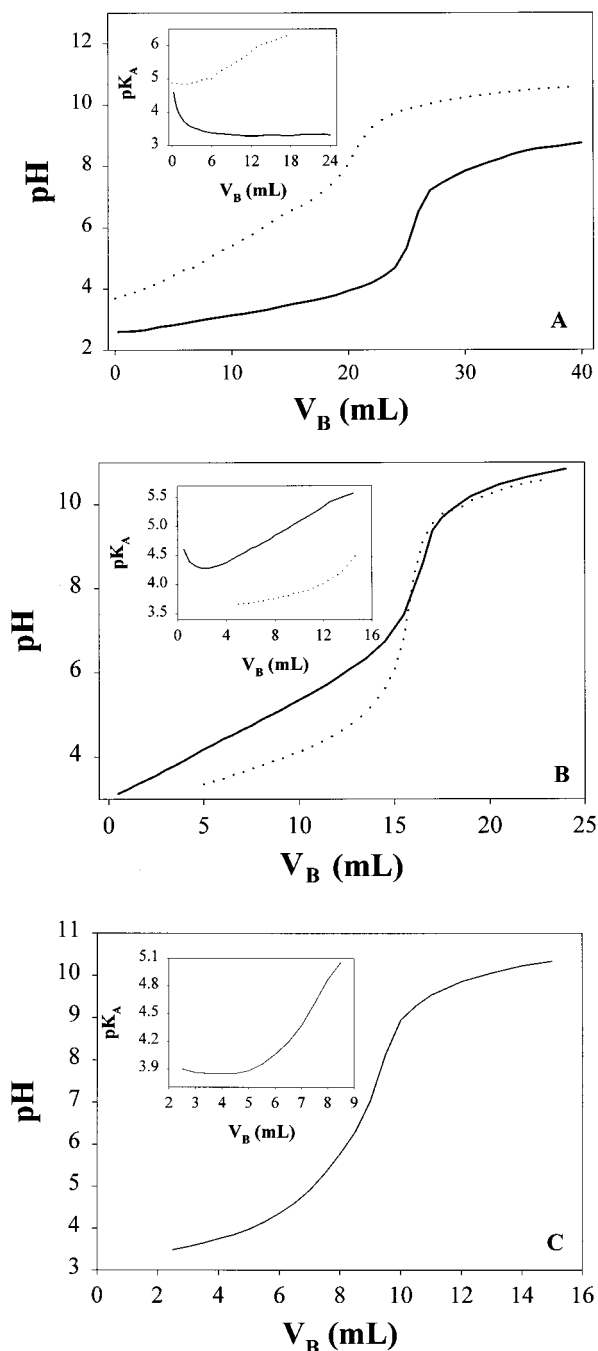


Figure 6. Titration curves and pK_A plots (insets) of tiopronin monomer and tiopronin-MPCs with strong base: (A) tiopronin monomer (—, apparent $pK_A = 3.5 \pm 0.33$) and 3 \times , RT preparation without supporting electrolyte (\cdots , apparent $pK_A = 5.56 \pm 0.53$); (B) 3 \times , RT preparation with 20 mM NaNO_3 (—, apparent $pK_A = 4.77 \pm 0.41$) and 3 \times , RT preparation with 1 M NaNO_3 (\cdots , apparent $pK_A = 3.95 \pm 0.27$); (C) $1/12\times$, RT preparation with 1 M NaNO_3 (apparent $pK_A = 4.10 \pm 0.42$). Titrations were performed by adding 0.1–0.5 mL aliquots of 2 mM NaOH to 2 mM solutions of the respective acid solutions in H_2O . pH was recorded initially and after each addition of base.

afterward was dialyzed without changing the pH. By so doing, any counterions associated with the adenosine groups of the CoA-MPCs would have remained following dialysis; no purity analysis in this regard was obtained. The CoA-MPCs have a powdery consistency, like tiopronin-MPCs, but differ by being soluble in methanol and ethanol as well as in water.

Figure 7 shows a TEM image and Au core size histogram

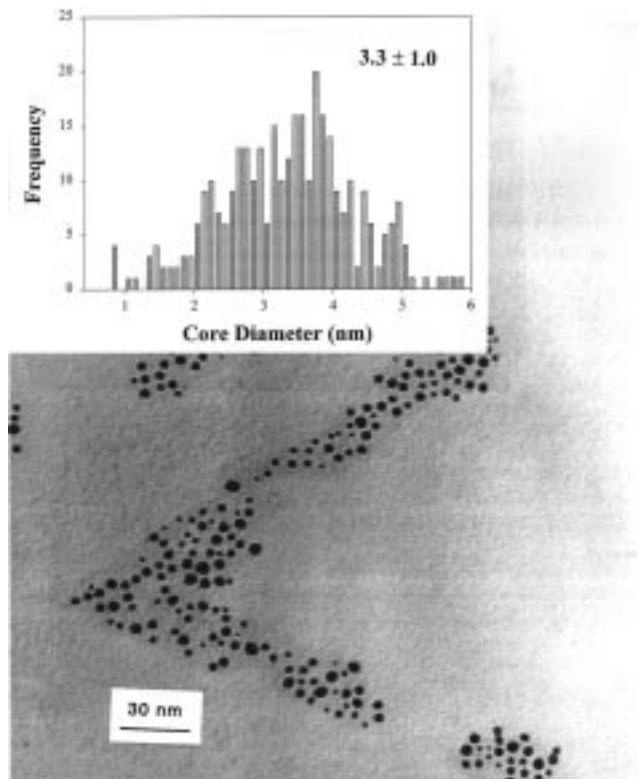


Figure 7. Transmission electron micrograph and core size histogram (inset) of CoA-MPC ($1/6\times$, RT). The average core diameter is given in inset.

(inset) of dialyzed CoA-MPC. The core size (3.3 ± 1.0 nm) of these clusters is similar to that of the larger tiopronin-MPCs (Table 1) but is somewhat smaller than that of alkanethiolate-MPCs prepared in toluene using similar thiol/gold reactant ratios.^{5b} For example, the two-phase synthesis of alkanethiolate-MPCs with the same Au:thiol ratio produced clusters with average core diameter ca. 4.4 nm.^{5b} This could be due to steric considerations as discussed above for the tiopronin-MPC system. The CoA-MPCs are quite polydisperse, with major populations centered at about 2.4 (~15%), 2.8 (~20%), 3.5 (~25%), 3.8 (~25%), and 5.0 nm (~10%). Assuming a truncated octahedral configuration as before, it appears (within the TEM resolution) that the formation of different populations of CoA-MPC sizes again tends to favor “magic” numbers of core Au atoms. Thermogravimetric analysis (TGA) gives 20.3% for the organic fraction, corresponding to an average of 84 CoA ligands per cluster and an effective projected footprint of about 0.56 nm^2 for each CoA ligand. This value is close to the calculated cross-sectional area of a CoASH molecule (0.62 nm^2), indicating a dense packing of the monolayer structure despite a sterically bulky headgroup.

The UV-vis spectrum of a CoA-MPC solution (Figure 8, solid line) shows a surface plasmon band centered at 518 nm. The similarity of this value to that found for alkanethiolate-MPCs^{5b} suggests somewhat surprisingly that the local dielectric environment of the Au core/monolayer interface of CoA-MPCs is not very different from that obtained with alkanethiolate-MPCs. The spectrum also shows a band at 259 nm which is due to the $\pi-\pi^*$ transition of the nucleotide end group (adenosine) of the CoA moiety and is expected for retention of the aromatic structure of the CoA ligand during the cluster synthesis. ^1H NMR spectra of CoA-MPCs (not shown) are also consistent with an intact CoA structure.

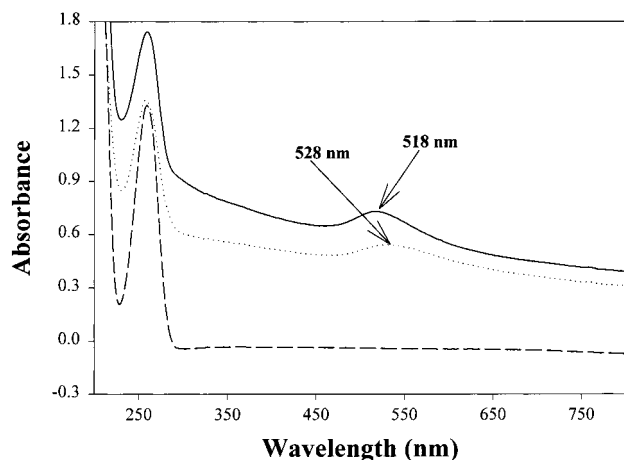


Figure 8. UV-vis spectra (in Tris buffer) of CoA-MPCs solutions: $1/6\times$, RT preparation, 3.6×10^{-6} M (based on MW = 320 kD) at pH = 1.27 (\cdots) and pH = 8.27 ($-$). UV-vis spectrum of CoASH monomer, 1.7×10^{-6} M ($- - -$).

The surface plasmon band in Figure 8 is pH sensitive. In a pH = 8.1 solution (solid line), the SP band position remains at 518 nm, but at pH = 1.27 (dotted line) shifts to 528 nm. This change parallels that seen for tiopronin-MPCs (Figure 4e), and shows that changes in the local dielectric environment can be prompted by acid-base charging of the ligand monolayer. Observations at very low pH values are complicated by the apparent instability

(gradual aggregation) of the clusters; it is well-known¹⁷ that coenzyme A contains bonds which are labile under acidic conditions.

Finally, titration of CoA-MPC solutions with a strong acid produces a pH profile (see Supporting Information) with a well-defined equivalence point, even in the absence of added electrolyte ($pK_A = 8.9$). The lack of significant broadening in the titration curve or drift of apparent pK_A without added electrolyte is likely due to the differences in effective ligand "chain length" compared to tiopronin. More specifically, the degree to which a ligand can seek rearrangement to minimize electrostatic repulsion effects depends jointly on the radius of curvature of the gold core and the chain length of the ligand.

Acknowledgment. This work was supported in part by grants from the National Science Foundation and Office of Naval Research. The authors thank Dr. Gary Pielak (UNC) for helpful discussions, Dr. Joseph DeSimone (UNC) for access to TGA equipment, and the UNC Dental Research Center for access to HRTEM measurements.

Supporting Information Available: Example HR-TEM images of the ($1\times$, RT), ($1/6\times$, RT), ($3\times$, 0 °C), and ($3\times$, 65 °C) preparations and accompanying core size histograms for the tiopronin-MPC samples and a titration curve for the CoA-MPC sample (7 pages). See any current masthead page for Internet access instructions.

LA9808420